https://doi.org/10.5194/egusphere-2026-865
Preprint. Discussion started: 10 April 2026

Mesoscale Structure of Flickering Aurora from Wide-Field High-Speed Imaging

Sota Nanjo[1], Satoshi Kurita[2], Tima Sergienko[1], Yoshizumi Miyoshi[3], and Ryuho Kataoka[4]

[1]Swedish Institute of Space Physics (IRF), Kiruna, Sweden
[2]Research Institute for Sustainable Humanosphere, Kyoto University, Kyoto, Japan
[3]Institute for Space–Earth Environmental Research, Nagoya University, Nagoya, Japan
[4]Okinawa Institute of Science and Technology, Okinawa, Japan

Correspondence: Sota Nanjo (sota.nanjo@irf.se)

Abstract. We report wide-field observations of flickering aurora obtained with a fast sCMOS camera and a diagonal fisheye lens at Poker Flat Research Range, Alaska, on 8 February 2016. The system recorded 512×512 pixel images at 80 Hz, enabling us to investigate the mesoscale organization of flickering along a discrete auroral arc over spatial scales of several hundred kilometers. Flickering occurred intermittently with dominant frequencies between 3 and 20 Hz, most commonly within a narrower band of 4–12 Hz. Spatial maps of the peak frequency reveal that regions with similar periodicities sometimes formed coherent clusters on scales of $\sim$10 km, and that multiple clusters with different frequencies (e.g., $\sim$8 and $\sim$13 Hz) could coexist simultaneously along the same arc, separated by $\sim$150 km. Some of these clusters moved together with the background arc, suggesting that the modulation is closely tied to the local plasma environment and inverted-V potential structures associated with discrete aurora. An automated patch detection analysis showed that, although individual events may locally suggest an inverse relationship between flickering frequency and patch size, this trend does not persist statistically. Instead, flickering at a given dominant frequency occurs over a wide range of patch sizes, with a typical north–south scale of 4.4 ± 2.4 km at 110 km altitude. These results are consistent with generation scenarios in which electron precipitation is modulated by interference among multiple EMIC waves in the auroral acceleration region, extending previous narrow-field studies to the mesoscale and demonstrating the diagnostic value of wide-field, high-cadence imaging for wave–particle interactions in the auroral ionosphere.

1 Introduction

Flickering aurora is an optical phenomenon in which luminosity rapidly oscillates at frequencies of approximately 3–15 Hz within localized, patch-like regions with horizontal scales of a few kilometers (Kataoka et al., 2021). These patches are known to appear below bright discrete auroras (Beach et al., 1968; Kunitake and Oguti, 1984) and may exhibit drifting or rotational motions (Kunitake and Oguti, 1984; Gustavsson et al., 2008). The amplitude of the luminosity modulation is typically about 10–20% of the brightness of the background discrete aurora (Lund et al., 1995; Sakanoi and Fukunishi, 2004; Gustavsson et al., 2008; Grydeland et al., 2008).

https://doi.org/10.5194/egusphere-2026-865
Preprint. Discussion started: 10 April 2026

Based on previous observational results, the origin of flickering aurora is widely regarded as being closely related to electron acceleration by electromagnetic ion cyclotron (EMIC) waves. Using simultaneous observations with sounding rockets and ground-based cameras, McFadden et al. (1987) reported field-aligned oscillations of the electron flux, known as field-aligned bursts (FABs), occurring simultaneously with flickering aurora. From the velocity dispersion of these electrons, they inferred that the source region was located at altitudes of approximately 4000–8000 km. It has been pointed out that the cyclotron frequencies of oxygen EMIC waves generated at these altitudes are in good agreement with the typical frequencies observed in flickering aurora (Temerin et al., 1986; Lund et al., 1995; Michell et al., 2012).

Several theoretical interpretations have been proposed to explain how EMIC waves accelerate electrons. Temerin et al. (1986) suggested that EMIC waves excited in the lower part of the acceleration region generate an ambipolar potential through the ponderomotive force. This potential transports cold electrons from the ionosphere upward to the lower part of the acceleration region, where the electrons subsequently resonate with the EMIC waves and are precipitated back into the ionosphere, leading to FABs. However, this model requires unrealistically large wave amplitudes. As an alternative scenario, McFadden et al. (1987) proposed that EMIC waves periodically perturb and release cold electrons trapped within the acceleration region, allowing them to be accelerated by the potential drop and precipitated into the ionosphere, thereby producing flickering aurora.

Sakanoi et al. (2005) demonstrated that the spatiotemporal patterns of flickering aurora observed with an imaging photometer can be explained by interference between two dispersive Alfvén waves (EMIC waves or inertial Alfvén waves), and showed that their results are consistent with the model proposed by Temerin et al. (1986), in which flickering aurora is generated through resonance between EMIC waves and electrons in the lower part of the acceleration region. In addition, Gustavsson et al. (2008) used numerical simulations to show that the complex spatiotemporal structures of flickering aurora can be reproduced by considering interference among multiple EMIC waves.

Within this theoretical framework, Whiter et al. (2010) observed chirps in which the flickering frequency varied on time scales of about 1 s, using narrow-field cameras and photometers. They suggested that higher flickering frequencies correspond to lower electron energies inferred from auroral emission intensity ratios, whereas lower frequencies are associated with higher electron energies. Their observations can be explained by the model of Chen et al. (2005), in which electron energy is primarily controlled by the parallel phase velocity of dispersive Alfén waves (such as EMIC waves), and are also consistent with the picture proposed by Temerin et al. (1986) and Sakanoi et al. (2005), in which electron flux is modulated through resonance between EMIC waves and electrons.

If EMIC waves excited at altitudes of several thousand kilometers are responsible for flickering aurora, then not only oxygen ion modes at frequencies of about 3–15 Hz but also higher-frequency modes associated with hydrogen and helium ions may be observable. In earlier periods, however, the temporal resolution of TV cameras was limited to 30 frames per second, making it difficult to record the rapid luminosity variations of flickering aurora in video. McHarg et al. (1998) overcame this limitation by performing photometric observations of flickering aurora at 40 kHz, and found amplitude modulations in the 35–60 Hz range, as well as fluctuation components reaching up to 180 Hz. With the advent of electron-multiplying CCD (EMCCD) detectors, Yaegashi et al. (2011) further demonstrated, using high-speed imaging at 100 Hz, that variations above 30 Hz were frequently observed, accounting for roughly one third of all events. Using multispectral EMCCD imaging, Kataoka

https://doi.org/10.5194/egusphere-2026-865
Preprint. Discussion started: 10 April 2026

et al. (2011) demonstrated fine-scale spatiotemporal variations of flickering aurora near the magnetic zenith and discussed their consistency with interference-based EMIC/DAW scenarios. More recently, using a scientific CMOS (sCMOS) camera, which provides higher-fidelity images without electron multiplication, Fukuda et al. (2017) conducted imaging observations at 160 frames per second and suggested that, in addition to patches flickering at typical frequencies of around 10 Hz, patch-like regions can also flicker over only a few frames (i.e., near 80 Hz). They interpreted this as the first evidence that flickering patches can be generated by multi-ion-mode EMIC waves.

As summarized above, a wide range of previous studies has suggested that interactions with EMIC waves play an essential role in the generation of flickering aurora and the accompanying FABs. However, the observational evidence used to construct these models has almost exclusively been obtained with narrow-field cameras. This is partly unavoidable for clearly resolving flickering patches, which are small-scale phenomena with horizontal sizes of a few kilometers and rapid intensity variations at frequencies of order 10 Hz, and for minimizing projection and line-of-sight superposition effects when characterizing small-scale structuring.

At the same time, there have been efforts to extend high-speed imaging to moderately larger fields of view (FoV). For example, Kataoka et al. (2015) used a $15^\circ \times 15^\circ$ high-speed camera oriented toward the magnetic zenith and reported compound auroral microstructures, including cases where localized flickering appeared together with pulsating aurora; they noted that the larger FoV was an important factor in identifying such simultaneous features.

Nevertheless, when the FoV is limited, it remains difficult to continuously follow flickering aurora over longer periods, particularly when it appears together with discrete auroral arcs that are narrow in the latitudinal direction and evolve dynamically. In this study, we successfully observed flickering aurora over a much wider FoV than in previous studies by using a ground-based camera equipped with a diagonal fisheye lens. While wide-FoV imaging provides improved contextual coverage, interpreting off-zenith (i.e., oblique) observations may require additional care because line-of-sight mixing can become more pronounced. We evaluate the consistency of our observations with existing generation models for flickering aurora and introduce newly revealed spatiotemporal characteristics: although individual examples may suggest a dispersion-like relationship between flickering frequency and patch size, this apparent trend does not persist statistically, implying that dispersion-like behavior inferred from generation models does not always translate directly into the optical signatures of flickering aurora.

2 Instruments

The detector used in the camera system was an ORCA-Flash 4.0 V2 manufactured by Hamamatsu Photonics. A NIKKOR 8 mm f/2.8 lens was employed, providing a diagonal FoV of 180°. No dedicated optical filters were used to block specific wavelengths. In this paper, we refer to this system simply as a scientific complementary metal–oxide–semiconductor (sCMOS) camera. The camera was installed at the Poker Flat Research Range, Alaska (65.12° N, 147.43° W), and oriented toward the geographic zenith. During the event analyzed in this study, images were recorded at 80 Hz with a frame size of 512×512 pixels. For the analyses presented after Figure 1, 2×2 software binning was applied to improve the signal-to-noise ratio, and the resulting 256×256 pixel images were used.

https://doi.org/10.5194/egusphere-2026-865
Preprint. Discussion started: 10 April 2026

2.1 Observation and analysis

Flickering aurora was observed with the sCMOS camera on 8 February 2016. Selected intervals of the observation are provided as Video 1 accompanying the electronic version of this paper to illustrate representative examples of flickering aurora (Nanjo, 2026). Figure 1 summarizes the event. Panel (a) shows a keogram constructed by extracting a vertical cross section at $x = 256$ pixels from each frame of the 512×512-pixel image sequence and stacking these cross sections in time. Panels (b)–(e) present all-sky images corresponding to the times indicated by the black arrows above panel (a).

The aurora initially appeared as a faint east–west arc around 06:20 UT (panel b). It subsequently intensified, developing into a typical discrete auroral arc by approximately 06:30 UT (panel c). From this period onward, localized, patch-like blinking areas became detectable within the arc on scales of several kilometers. The discrete arc and its associated flickering patches remained within the FoV for about one hour, exhibiting temporal variations in their average brightness, and eventually faded after 07:00 UT as a bulge-like bright auroral structure propagated westward. During the event, the magnetic coordinates of the observation site were approximately $65.3°$ MLAT and 19.2–20.0 MLT.

Panel (f) shows the sum of spectra obtained by applying the fast Fourier transform (FFT) for every 4-s window to the pixels within the region outlined by the black dashed line in panel (b). From around 06:30 UT, when the aurora began to brighten, intervals of enhanced power appeared intermittently in the frequency range from a few hertz up to about 20 Hz. The frequencies exhibiting high power were broadly consistent with previous studies (Kataoka et al., 2021). However, the occurrence of flickering was intermittent, and the dominant frequencies varied with time.

At 06:34–06:39 UT, 06:43–06:45 UT, and 06:52–06:55 UT (intervals indicated by white arrows), the signals in this frequency band dropped to the noise level. This occurred because the background discrete aurora weakened, reducing the amplitude of the flickering to a level at which it was no longer detectable as a signal. Weak flickering can nevertheless be identified in Video 1. Around 06:58–07:02 UT, the arc propagated equatorward and narrowed in its north–south extent, forming a typical curtain-like aurora just before the substorm onset. During this interval, no flickering was detected on the arc. However, flickering was observed in a latitudinally broader discrete aurora that appeared in a region farther north, as well as in the bulge observed afterward.

To investigate spatial variations in the periodicity, we examined the frequency distribution within a one-second interval. Figure 2 presents the results for the one-second interval starting at 06:50:34.5 UT (Figure 1d), during which flickering aurora was clearly observed. The grayscale background image represents the average of the 80 frames acquired during this one-second period. The fast Fourier transform (FFT) was applied to the one-second time series at each pixel whose mean count exceeded a predefined threshold, indicating the presence of auroral emissions. Among these spectra, pixels for which the spectral power in the 3–20 Hz range exceeded a threshold determined by visual inspection were identified as exhibiting flickering. For these pixels, the frequency corresponding to the maximum amplitude is shown in color.

Flickering was detected over broad portions of the arc, although not uniformly across its entire extent. This spatially intermittent pattern is consistent with visual inspection. The dominant frequencies varied spatially, generally ranging from 5 to 15 Hz. The distribution was not completely random: in some regions extending over more than 10 km, spatially coherent clus-

https://doi.org/10.5194/egusphere-2026-865
Preprint. Discussion started: 10 April 2026

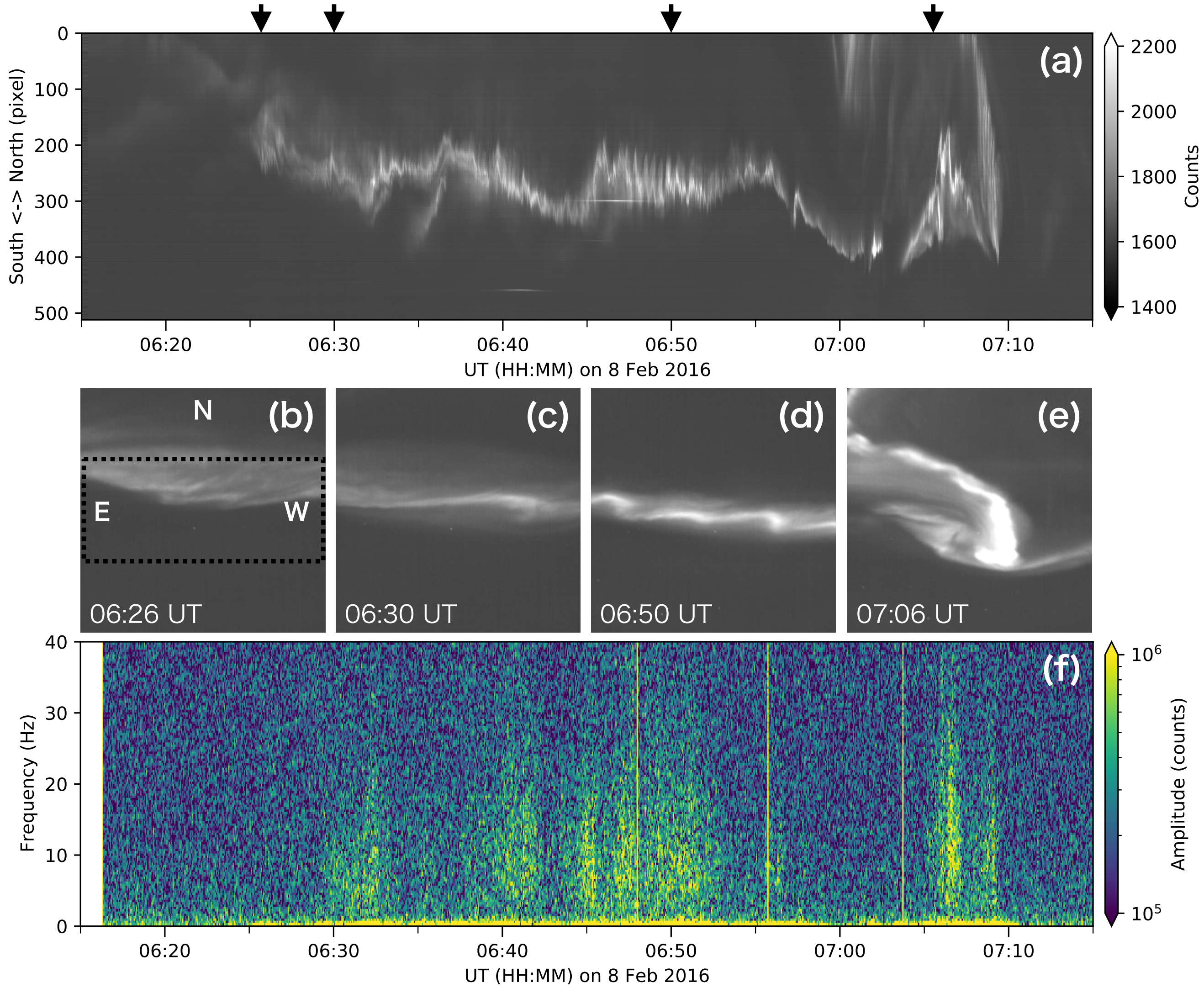

Figure 1. (a) Keogram constructed from the sCMOS camera images on 8 February 2016. (b–e) Selected all-sky images at the times indicated by the arrows in (a). (f) Sum of FFT spectra for the region outlined in (b), showing intermittent enhancements in the 3–20 Hz range associated with flickering aurora.

https://doi.org/10.5194/egusphere-2026-865
Preprint. Discussion started: 10 April 2026

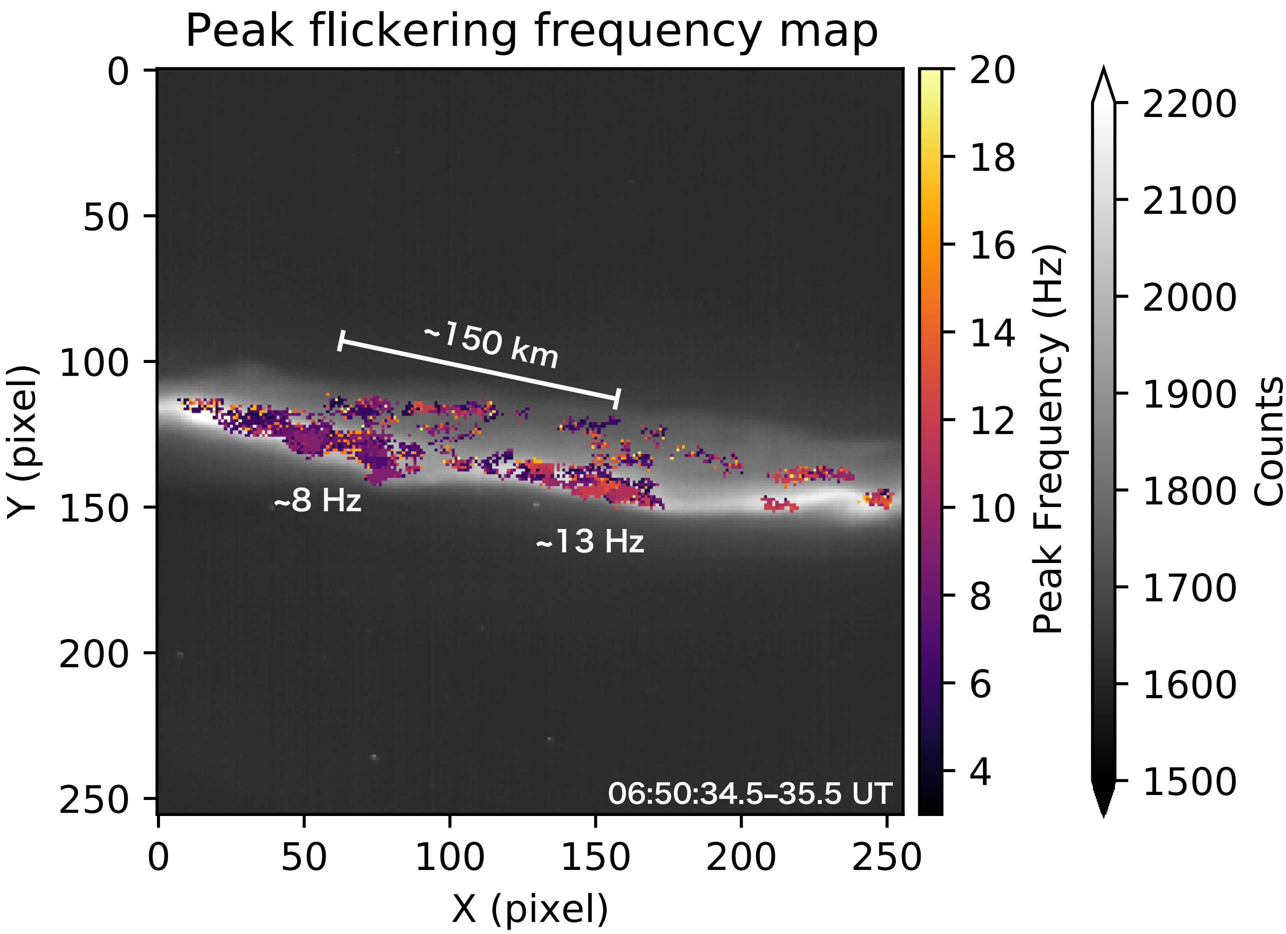

Figure 2. Spatial distribution of the dominant flickering frequency for the one-second interval starting at 06:50:34.5 UT. The color indicates the peak frequency in the 3–20 Hz range at pixels where the FFT power exceeds a threshold.

ters exhibited similar peak frequencies. These clusters were larger than individual flickering patches; that is, multiple patches sharing similar frequencies formed a single cluster. In Figure 2, for example, frequencies around $\sim$8 Hz were prevalent in regions with x-coordinates below $\sim$80, whereas frequencies around $\sim$13 Hz were more common in regions with x-coordinates above $\sim$120. The separation between these two regions was approximately 150 km, assuming an emission altitude of 110 km.

As shown in Figure 3, clusters at a given peak frequency were sometimes observed to move together with the background auroral arc. Panel (a) shows the average of 80 images acquired during a one-second interval starting at 06:50:20.0 UT. An arc extending in the east–west direction is visible; although the flickering cannot be discerned from the still image, the luminosity modulation is clearly seen in Video 1. The FFT was applied to the time series obtained during this one-second interval at each pixel, and, as in Figure 2, the frequency with the maximum amplitude in the 3–20 Hz range is shown in panel (b). Panels (c) and (d) show the same analyses applied to data acquired four seconds later, corresponding to panels (a) and (b), respectively.

https://doi.org/10.5194/egusphere-2026-865
Preprint. Discussion started: 10 April 2026

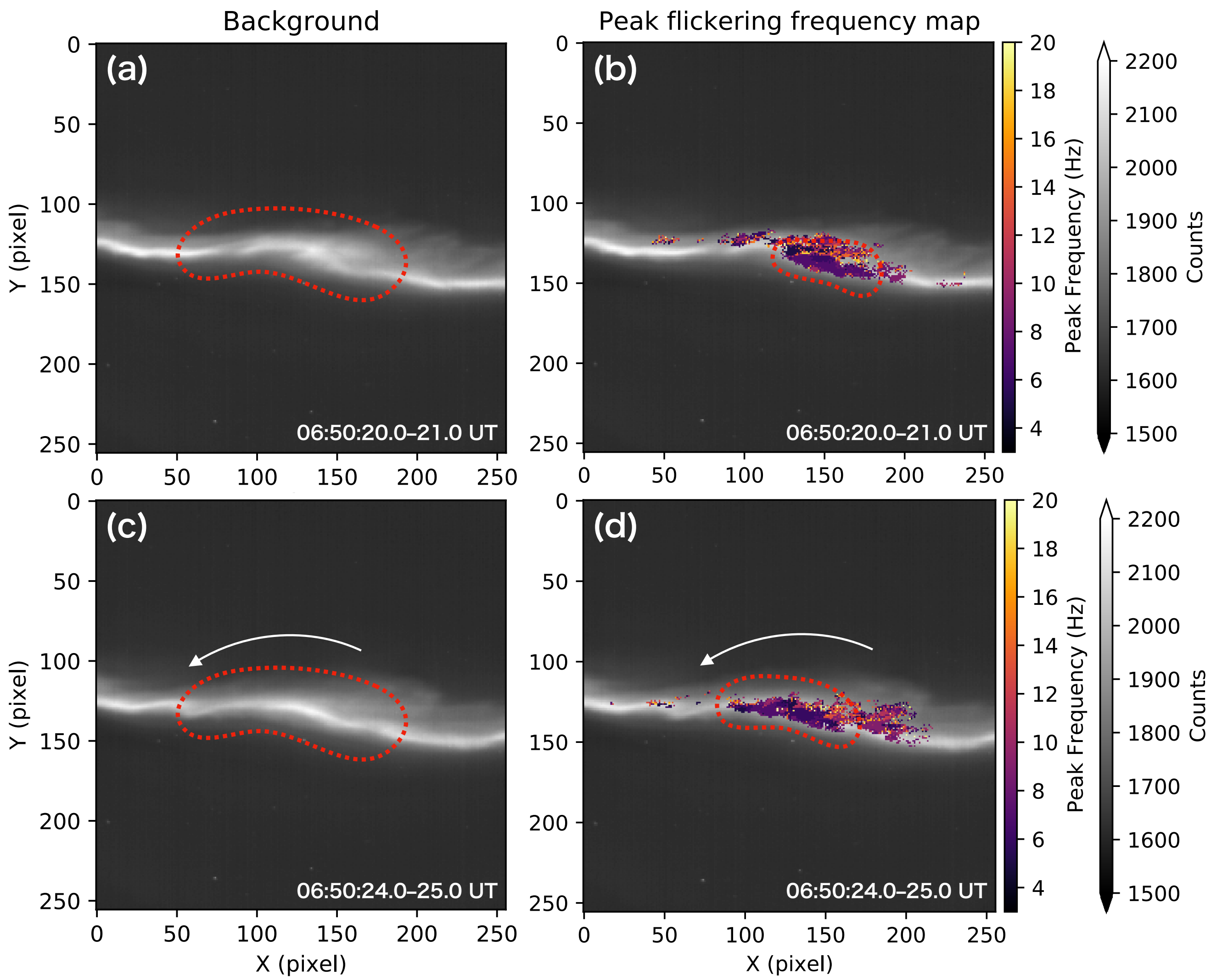

Figure 3. Spatiotemporal evolution of flickering-frequency clusters associated with an auroral arc. (a) Average of 80 images over a one-second interval starting at 06:50:20.0 UT. (b) Spatial distribution of the peak flickering frequency (3–20 Hz) derived from FFT. (c, d) Same as (a) and (b), respectively, but for data acquired four seconds later.

Comparing panels (a) and (c) of Figure 3, an eastward propagation is evident in the region enclosed by the red dotted line, in the direction indicated by the white arrow in panel (c). Specifically, a slightly folded, twisted structure becomes more linear in panel (c). At the same time, comparison of panels (b) and (d) shows that the 7–8 Hz cluster corresponding to this folded structure (outlined by the red dotted line in panel (b)) shifted eastward in concert with the motion of the auroral arc.

In the analyses presented so far, frequency analysis was performed on a pixel-by-pixel basis, without explicitly considering individual patch structures. However, to systematically investigate the relationship between patch size and periodicity, it is

https://doi.org/10.5194/egusphere-2026-865
Preprint. Discussion started: 10 April 2026

necessary to automatically detect the flickering patches themselves. Although two-dimensional region extraction directly from the video data is in principle possible, no optical filter was used in the present observations. As a result, the strong 557.7 nm oxygen emission can blur the boundaries of flickering patches, potentially introducing uncertainty in the estimated patch sizes. Therefore, in this study, patch detection was performed using keograms constructed from the video data. This approach has several limitations: a keogram cross section does not necessarily pass through the center of every patch, and off-zenith viewing may increase line-of-sight superposition that can further complicate the apparent patch morphology. Nevertheless, keograms offer the practical advantage that even when the brightening of a single patch persists over multiple frames, it can be continuously tracked as a single patch. In this study, we prioritized this advantage.

Figure 4 illustrates the workflow for the automatic detection of flickering patches. As an example, we show a relatively stable interval with little motion, observed over a 23 s period starting at 06:50:15 UT. Panel (a) shows a keogram extracted at $x = 150$. Fine vertical stripe structures on time scales shorter than 1 s are visible over much of the panel (minor ticks on the horizontal axis are given at 1 s intervals); these stripes represent the luminosity modulation of flickering aurora, and our first goal is to measure their vertical extent.

Panel (b) is obtained by removing dark regions in panel (a) using a threshold and subtracting a 0.5 s moving average from the remaining regions, thereby enhancing the high-frequency variations. Panel (c) shows a binary image derived from panel (b), where regions with ΔCount exceeding 30 are set to 1 and the others to 0. Structures extending over more than four pixels in the vertical direction are detected and overlaid with red lines. Each red line corresponds to the length of an individual patch. Although not all structures are detected, the threshold for ΔCount was intentionally set high in order to reduce false positives.

Panel (d) shows the frequency with the maximum amplitude obtained by applying the FFT to the time series extracted from panel (b) at 2 s intervals. The time windows were shifted in steps of 0.2 s, resulting in overlapping segments. Regions with small amplitudes (i.e., low brightness) were regarded as non-flickering and are left blank.

Comparison of panels (a) and (c) shows that, although not all flickering structures are detected, the identified structures (highlighted in red in Figure 4(c)) correspond to the bright phases of the flickering and their lengths are generally consistent with the structures seen in panel (a). Furthermore, comparison of panels (c) and (d) indicates that, as illustrated in the figure, relatively long patches in the y-direction (corresponding to about 7–10 km at an altitude of 110 km) were observed during the earlier part of the interval (approximately 18–24 s), when the peak frequency was around 8 Hz. In contrast, during the later intervals (approximately 29–32 s and 36–38 s), shorter patches (about 4–6 km at an altitude of 110 km) were detected, with corresponding frequencies of about 12 Hz. In other words, larger patches tended to exhibit longer flickering periods (i.e., lower frequencies).

The same analysis as that shown in Figure 4 was also applied to a brighter and more dynamically evolving discrete aurora observed during a 23 s interval starting at 07:06:17 UT (corresponding to Figure 1e). The results are presented in Figure 5. The figure format and analysis procedure are the same as in Figure 4; however, note that the range of the y-axis and the color-map scales in panels (a) and (b) are slightly different.

As shown in Figure 5(a), compared with Figure 4(a), the aurora occupied a much broader region, and flickering was correspondingly observed over a wider area. During the earlier part of the interval, two structures with comparable background

https://doi.org/10.5194/egusphere-2026-865
Preprint. Discussion started: 10 April 2026

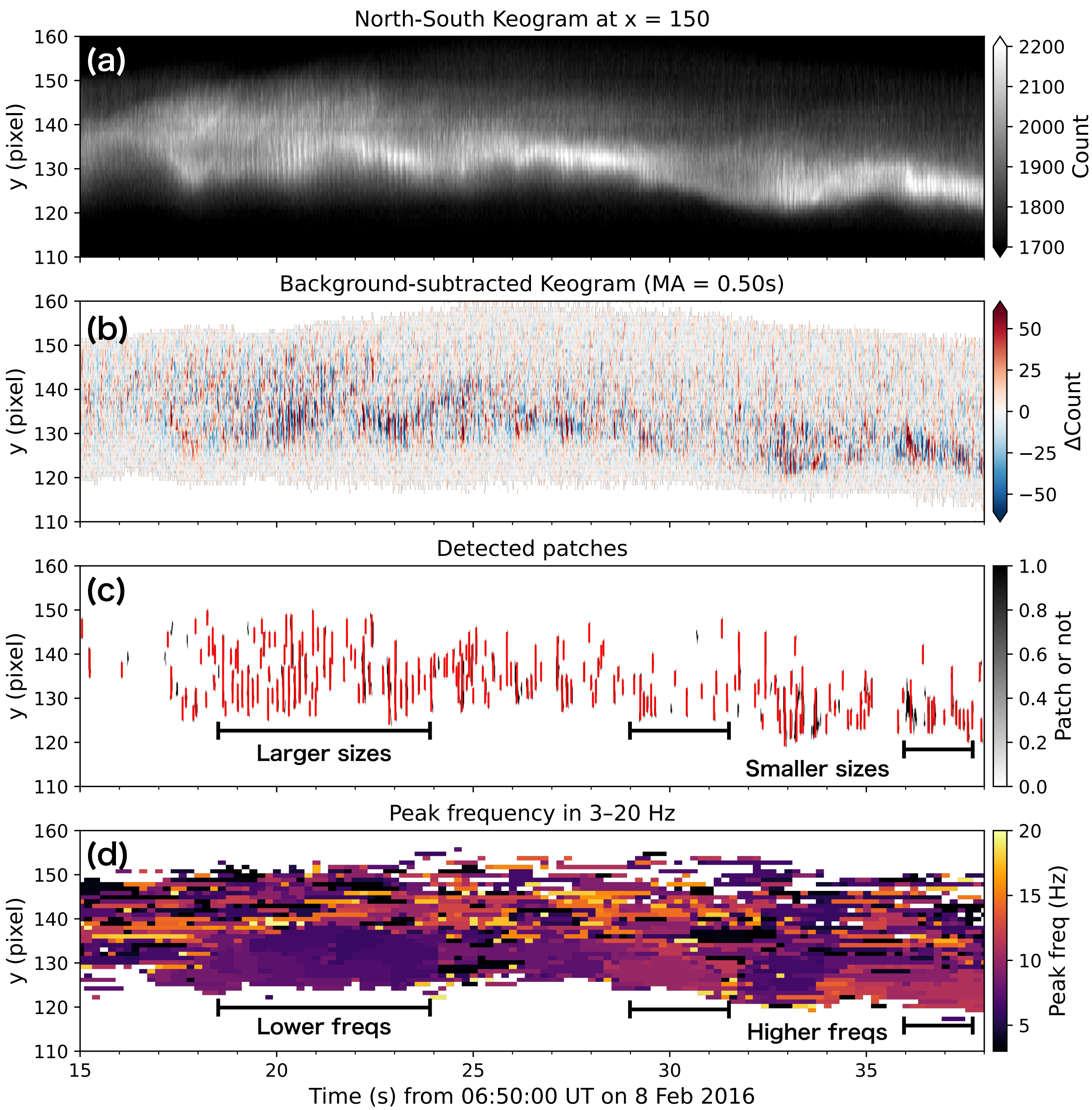

Figure 4. Workflow for the automatic detection of flickering patches, illustrated using a relatively stable 23 s interval starting at 06:50:15 UT. (a) Keogram extracted at $x = 150$, showing vertical stripe structures associated with flickering luminosity modulation. (b) High-frequency variations enhanced by thresholding and subtraction of a 0.5 s moving average. (c) Binary detection of flickering patches (ΔCount > 30), with patch lengths identified by red lines. (d) Peak flickering frequency obtained from FFT analysis of the time series in (b).

https://doi.org/10.5194/egusphere-2026-865
Preprint. Discussion started: 10 April 2026

brightness were observed above and below (north and south of) $y \approx 125$ pixels. In the region enclosed by the red dotted line, the flickering patches appeared at relatively long intervals, corresponding to a frequency of about 4 Hz as seen in panel (d). The patch sizes in this region were typically about 7–11 km at an altitude of 110 km.

At the same time, in the region enclosed by the blue dotted line, located approximately 20 km away, the patches flickered at much shorter intervals, with a corresponding frequency of about 14 Hz in panel (d), roughly three times higher than in the red region. The patch sizes in this region were mostly about 3–5 km, representing roughly a factor-of-two difference compared with the red region. The tendency for larger patches to exhibit longer flickering periods (lower frequencies) is consistent with the results shown in Figure 4.

In Figure 5(a), during a few seconds starting at 07:06:22 UT, structures extending toward the upper right were observed three times, as indicated by the black arrows. From the inclination of these structures, it can be inferred that the bright portion of the aurora propagated from south to north at a speed of approximately 10 km s^{-1}. Figures 5(b) and 5(c) show that, even as these bright regions moved, flickering continued to accompany them. However, the patches themselves did not remain continuously bright while drifting northward.

In Figure 5(d), a region in which the peak frequency remains nearly constant along an upward-rightward trend can be identified, as outlined by the white dotted line. Although such a region does not correspond one-to-one with the structures seen in Figure 5(a), they may indicate that the flickering period is not strongly modulated during the propagation of the discrete aurora.

After the interval during which north–south-propagating auroral structures were observed (after 07:06:25 UT), patches with a wide range of sizes, from approximately 2 to 15 km, were detected. Correspondingly, the peak-frequency panel in Figure 5(d) shows a broad distribution of values ranging from about 3 to 20 Hz. In contrast to the period up to 07:06:22 UT and the cases shown in Figure 4, it was difficult to identify a systematic relationship between patch size and frequency during this later interval. Even when focusing on individual moments, multiple isolated patches sometimes appeared without continuity in the north–south direction.

In addition, as indicated by the black arrows in Figure 5(b), patch structures resembling a laterally reversed J shape were observed. This implies that the patches propagated in the north–south direction at speeds of up to approximately 30 km s^{-1}, rather than expanding from a fixed point. Although not shown in the figures, numerous patches propagating in the east–west direction were also identified in Video 1.

We statistically examined the relationship between the north–south extent of patches and their flickering frequency observed in Figures 4 and 5. Specifically, for the software-binned 256×256 pixel image sequences, the same analysis as in Figures 4 and 5 was applied at x-coordinates from 25 to 250 in steps of 25 pixels, at one-minute intervals over the period from 06:20 to 07:10 UT. For each analysis window, the length of each patch (in pixels) obtained from panel (c) was associated with the corresponding peak frequency from the frequency map in panel (d), yielding pairs of patch length and peak frequency. The patch lengths were then converted to physical distances at an assumed altitude of 110 km.

Figure 6 shows the occurrence frequency map of the inverse of the north–south patch length at an altitude of 110 km and the corresponding peak flickering frequency, based on the 23,704 patches obtained through the procedure described above. In

https://doi.org/10.5194/egusphere-2026-865
Preprint. Discussion started: 10 April 2026

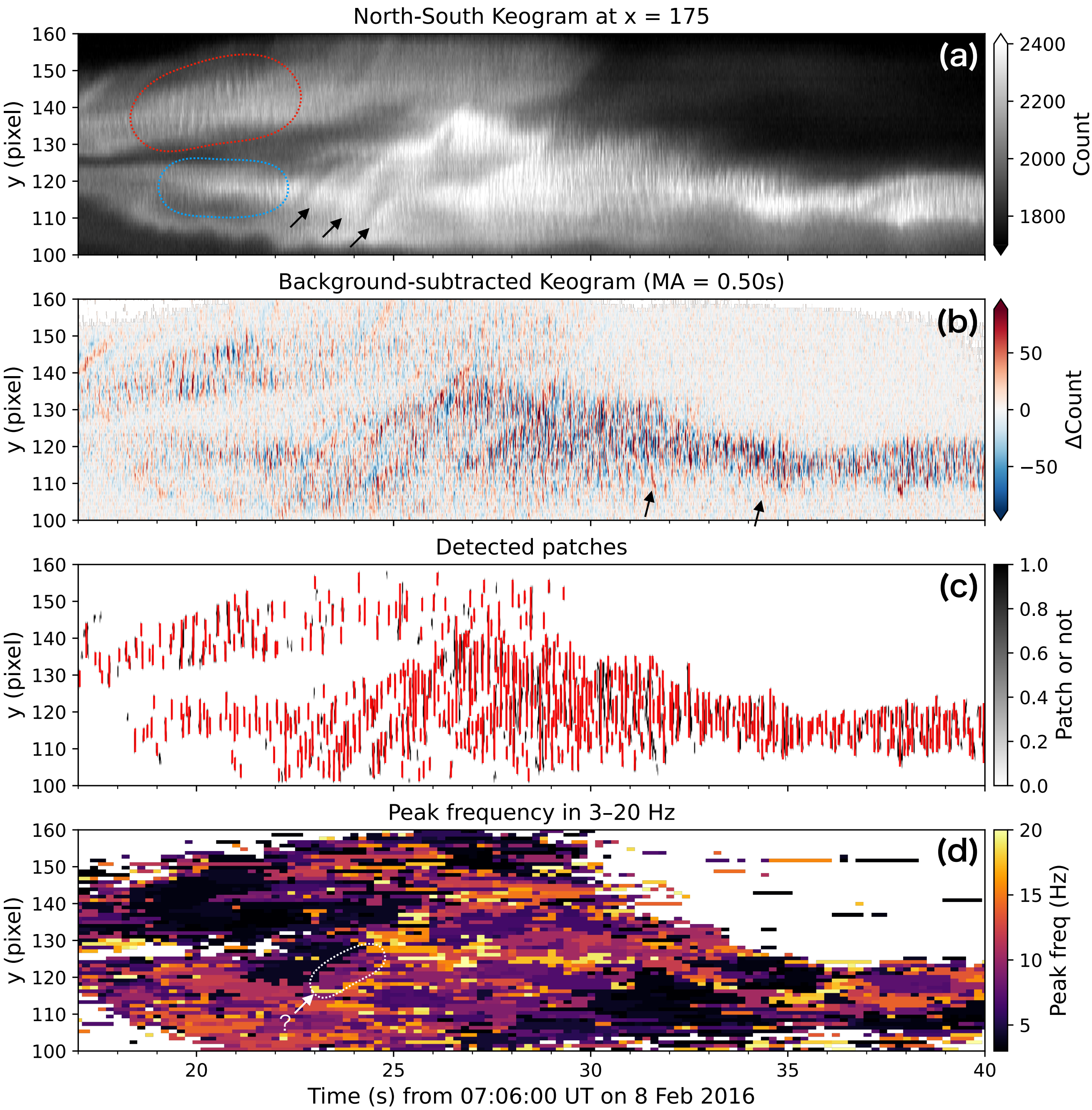

Figure 5. Same analysis as in Figure 4 applied to a brighter, more dynamically evolving discrete aurora during a 23 s interval starting at 07:06:17 UT (see Figure 1e). Panels (a)–(d) follow the same format as Figure 4, with slightly different y-axis and color-map ranges.

https://doi.org/10.5194/egusphere-2026-865
Preprint. Discussion started: 10 April 2026

the figure, the mean value and the $\pm 1\sigma$ range for each bin on the horizontal axis are indicated by white solid and dashed lines, respectively. According to Figure 6, the flickering frequency remains nearly constant at about 8 ± 4 Hz, regardless of patch size. Although the examples shown in Figures 4 and 5 suggested a tendency for larger patches to exhibit lower frequencies (i.e., longer flickering periods), this trend is not reproduced statistically. This result is unchanged even when the analysis is restricted to shorter time intervals; that is, patch size does not depend on the flickering period over time. The typical north–south patch size is 4.4 ± 2.4 km.

The inverse patch size shows a pattern of repeated local minima and maxima, particularly on the right-hand side of the distribution (corresponding to smaller patch sizes); however, this behavior is an artifact of the analysis arising from the fact that the spatial resolution of the observations is lower than the bin resolution along the horizontal axis.

The absence of a statistical relationship between flickering frequency and patch size suggests that the observed optical scale does not directly reflect a simple single-mode dispersion relation. Instead, it is naturally interpreted in terms of interference among multiple EMIC waves, as proposed in previous studies (Sakanoi et al., 2005; Gustavsson et al., 2008).

2.2 Discussion

We analyzed a flickering aurora event observed above the Poker Flat Research Range, Alaska, during the interval from approximately 06:20 to 07:10 UT on 8 February 2016. The main results can be summarized as follows:

- Flickering occurred intermittently in both space and time over a frequency range of 3–20 Hz.
- Flickering patches at similar frequencies sometimes formed spatial clusters extending over regions larger than 10 km.
- Some of these frequency clusters moved together with the background auroral arc.
- Although individual patch analyses locally suggested a tendency for larger patches to exhibit lower frequencies, this trend was not confirmed statistically.
- These results provide mesoscale observational support for interference-based EMIC/DAW generation scenarios, extending previous narrow-FoV interpretations to spatial scales of several hundred kilometers.

The flickering frequencies observed in this study are generally consistent with values reported in previous studies (e.g., Gustavsson et al., 2008; Michell et al., 2012; Sakanoi and Fukunishi, 2004; Whiter et al., 2010). These frequencies are not inconsistent with models in which flickering aurora originates from O^+-mode EMIC waves excited at altitudes of approximately 4000–8000 km (Temerin et al., 1986; McFadden et al., 1987). Variations at frequencies higher than 30 Hz, which were discussed by McHarg et al. (1998), Yaegashi et al. (2011), and Fukuda et al. (2017), are close to the Nyquist frequency of the present observations (40 Hz) and are therefore difficult to measure reliably; accordingly, they are not discussed in this paper.

The spatiotemporal variation in the presence or absence of flickering may provide insight into the conditions under which flickering becomes visible, and by extension into the excitation conditions of EMIC waves. As shown in Figure 1, flickering disappeared as the auroral arc propagated equatorward (southward) toward substorm onset while both weakening in brightness

https://doi.org/10.5194/egusphere-2026-865
Preprint. Discussion started: 10 April 2026

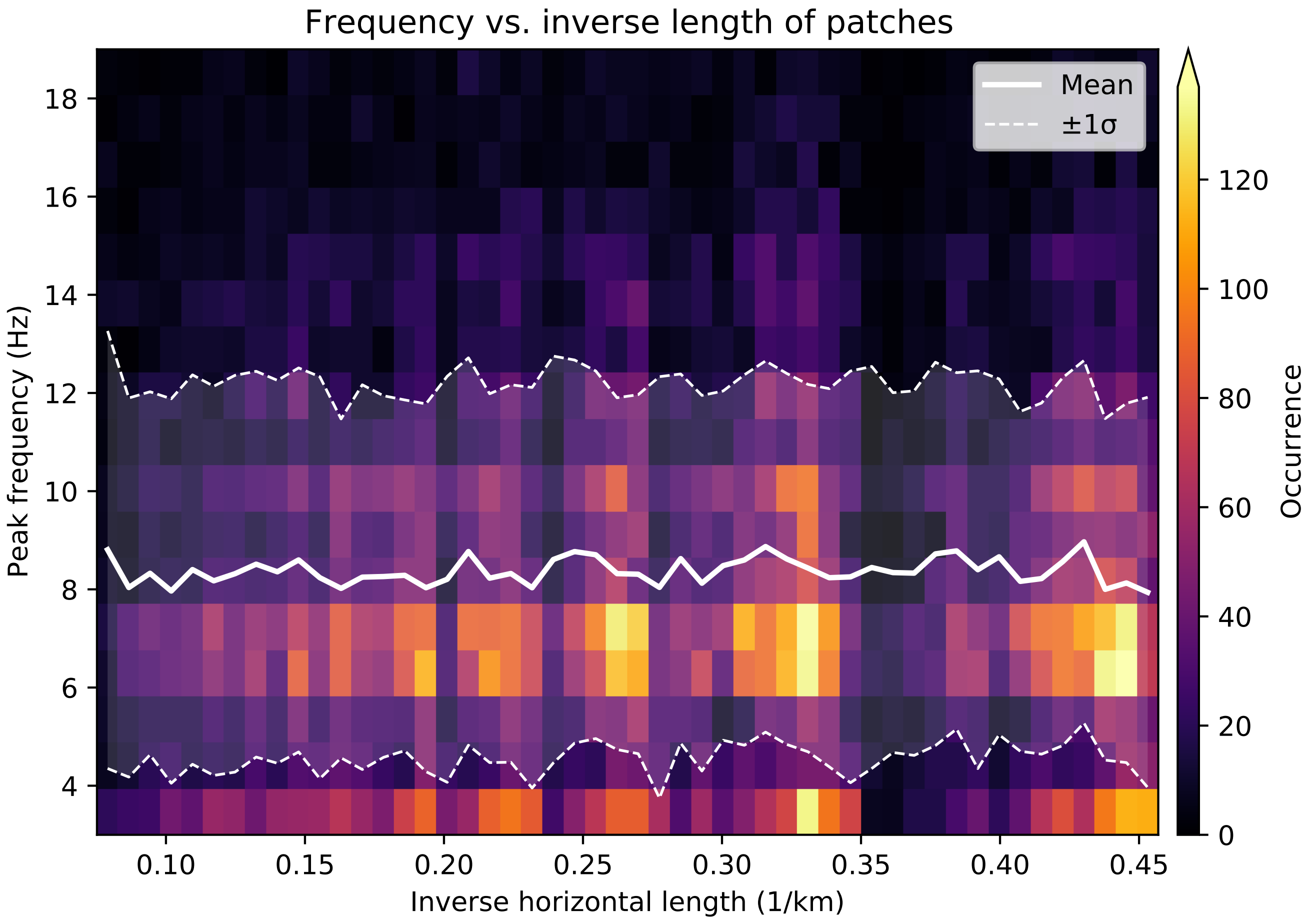

Figure 6. Statistical relationship between flickering frequency and patch size. The occurrence frequency map shows the peak flickering frequency as a function of the inverse north–south patch length at an assumed altitude of 110 km, based on 23,704 detected patches. White solid and dashed lines indicate the mean value and the $\pm 1\sigma$ range for each bin, respectively.

https://doi.org/10.5194/egusphere-2026-865
Preprint. Discussion started: 10 April 2026

and narrowing in latitudinal extent; the same was true even when the brightness increased sharply just before onset. In contrast, during the same interval, flickering accompanied a relatively bright, latitudinally broader discrete aurora that appeared on the poleward (northward) side.

These observational results suggest that, while a certain level of background discrete auroral brightness is favorable for the visibility of flickering, flickering does not necessarily occur most readily in the brightest discrete aurora. They also indicate that a broader latitudinal extent of the background discrete aurora may be one of the conditions required for flickering aurora to be observable.

One possible growth mechanism for EMIC waves that may drive flickering aurora is a beam-driven instability associated with precipitating auroral electrons (e.g., Temerin and Lysak, 1984; Lin et al., 1989). In this framework, the wave growth rate depends on a variety of parameters, including the temperature and density of the electron beam and the background electron density (see equation (11) in Temerin and Lysak, 1984). Considering our observations, it is possible that the relevant parameters initially lay within a range favorable for EMIC growth, but that as substorm onset approached, for example, the background electron density became too high, reducing the growth rate so that flickering became undetectable.

It should also be noted that in the growth theory of Temerin and Lysak (1984), EMIC wave growth is controlled primarily by propagation along the magnetic field line, and perpendicular (vertical) propagation is not emphasized. Therefore, the apparent disappearance of flickering when the arc becomes latitudinally narrow may simply coincide with a period when the background arc weakened and the flickering amplitude became too small to detect, rather than indicating a direct causal relationship. It should also be noted that this linear growth model cannot account for the large amplitudes of observed O^+ EMIC waves; Lund and LaBelle (1997) suggested that nonlinear or inhomogeneous effects may be important.

According to Temerin et al. (1986), flickering aurora can be produced when EMIC waves in/below the main acceleration region carry a finite parallel electric field that induces an oscillatory motion of low-energy electrons; if the oscillation velocity becomes comparable to the wave's parallel phase velocity, electrons can stay in phase with the wave and be accelerated downward, modulating the field-aligned flux at the wave frequency. They also showed that the parallel phase velocity of EMIC waves depends sensitively on the plasma density distribution along the magnetic field line, so that regions of lower density provide more favorable conditions for such wave–particle interaction.

In the present event, the temporal variation in the presence or absence of flickering should not be attributed solely to changes in the EMIC wave growth rate. It also reflects variations in the parameters required for resonant acceleration, as well as changes in the supply of low-energy electrons, associated with the spatiotemporal evolution of the discrete arc. For example, as onset approached, changes in the plasma distribution around the acceleration region may have shifted the parallel phase velocity of EMIC waves and the altitude at which the parallel electric field peaks, making resonant acceleration less effective along field lines in the equatorward onset arc, while the resonance condition may have been maintained along field lines connected to the broader and poleward discrete aurora.

Figure 2 shows that, at the same time, two regions along the same discrete arc exhibited coherent flickering at clearly different peak frequencies, around 8 Hz and around 13 Hz, with a horizontal separation of $\sim$150 km at an assumed altitude of 110 km.

https://doi.org/10.5194/egusphere-2026-865
Preprint. Discussion started: 10 April 2026

In addition to these two frequency bands, smaller-scale regions with a variety of flickering frequencies were scattered along the entire arc.

In the framework proposed by Sakanoi et al. (2005), flickering aurora is produced when dispersive Alfvén/EMIC waves emitted from a localized source region are confined within a resonance cone and form standing or interfering wave patterns, which then map to patches or columns a few kilometers across in the ionosphere. The ∼150 km separation between the two main frequency bands in Figure 2 is therefore difficult to reconcile with the idea that all of the observed flickering arises from a single resonance cone fed by a single localized source; the distance is more than an order of magnitude larger than the typical size of an individual flickering patch. A more natural interpretation is that multiple wave sources are distributed along the arc in the east–west direction, each sampling slightly different local plasma conditions (electron density, temperature, ion composition, and field–aligned potentials) and therefore developing its own preferred modulation frequency through differences in EMIC/DAW growth rate and electron resonance conditions.

The observed frequency differences can also be interpreted in terms of variations in the source altitude. If the dominant flickering frequency is primarily controlled by the local ion cyclotron frequency of the relevant EMIC mode, $f_{\mathrm{ci}} = qB/(2\pi m)$, then a given frequency band corresponds to a specific range of magnetic field strength $|B|$ along the magnetic field line. Using the IGRF model, O^+ cyclotron frequencies of 8 Hz and 13 Hz are estimated to correspond to source altitudes of approximately 6000 km and 3800 km, respectively, above the observation site. This implies that the two main frequency bands observed in Figure 2 could originate from EMIC waves generated at different heights along neighboring field lines that map to the same auroral arc.

The simultaneous appearance of flickering patches with different peak frequencies was also confirmed during the interval enclosed by the red and blue dotted lines in Figure 5(a). In this case, a region of reduced auroral luminosity, appearing dark in the keogram, was present between the two flickering areas, indicating that each area corresponds to a separate inverted-V potential structure. This may imply that different wave source regions can coexist while being spatially separated, even on scales of only ∼20 km at ionospheric altitudes.

Furthermore, the two regions exhibited dominant frequencies of approximately 4 Hz and 14 Hz, respectively, differing by roughly a factor of three. This suggests that, even at such close spatial separations, local variations in plasma parameters, such as electron density, ion composition, and current system, can strongly influence the growth and resonance conditions of EMIC waves, thereby producing substantial differences in the observed flickering frequencies.

Figure 3 shows that frequency clusters can move in concert with the background arc. This result suggests that the frequencies of EMIC waves driving flickering are not uniquely determined by large-scale spatial parameters such as magnetic latitude or L shell, but are instead strongly tied to the inverted-V potential structures present at a given time and to the local plasma environment associated with the accompanying discrete aurora. As demonstrated in Figures 2 and 5, multiple wave source regions can coexist along the arc in the east–west direction, exhibiting markedly different peak frequencies at different locations. The results in Figure 3 further indicate that these wave source regions can migrate collectively as the background auroral arc evolves and moves.

https://doi.org/10.5194/egusphere-2026-865
Preprint. Discussion started: 10 April 2026

In other words, the visibility of flickering aurora likely depends not only on the presence of localized EMIC wave sources along magnetic field lines, but also critically on the structure and temporal evolution of the inverted-V potentials and the associated discrete auroral arcs that host these sources. This interpretation is consistent with the idea proposed by Sakanoi et al. (2005), in which flickering aurora is generated by EMIC/IAW closely linked to inverted-V electron precipitation in the auroral acceleration region, and extends that picture by providing mesoscale observational evidence that multiple interference-driven wave source regions can coexist and migrate along a single discrete auroral arc.

In Figure 4 and in the early phase of Figure 5, when the spatial structure of the background auroral arc was relatively stable, larger patches appeared to be associated with lower flickering frequencies. This behavior hints at a possible correspondence between the flickering frequency f and the perpendicular wave number $k_\perp$ expected from the dispersion relation of obliquely propagating EMIC waves. Indeed, Yaegashi et al. (2011) examined the relationship between frequency and apparent wave number derived from optical observations and compared it with the dispersion relation of O^+ EMIC waves (their equation (7) and Figure 7), showing that the observations are broadly consistent with the theoretical curve at frequencies below 15 Hz.

Motivated by these results, we also investigated the statistical relationship between patch size and flickering frequency in Figure 6. However, no clear tendency for larger patches to correspond to lower frequencies was identified; instead, flickering occurred over a wide range of patch sizes within the frequency band of 4–12 Hz. We note that the present analysis may be affected by off-zenith viewing, where integration along the line of sight can cause multiple flickering components to be mixed within a single pixel and the apparent periodicity to become less stable. Since we use only the FFT peak frequency as a summary metric, it is unlikely that this effect strongly distorts the overall frequency–size distribution; however, it cannot be completely neglected and may contribute to additional scatter.

This result is not necessarily inconsistent with generation models involving EMIC/DAW waves. In the Sakanoi–Temerin model, flickering aurora is interpreted as arising not from a single wave but from the interference of multiple EMIC/DAW waves. As a result, a simple relationship derived from the dispersion relation is not guaranteed to be directly reflected in the observed optical patch structures. Indeed, Figure 7 of Yaegashi et al. (2011) shows that patches with broadband frequency characteristics exhibit widely scattered representative frequencies, such that the relationship between f and $k_\perp$ is not uniquely defined. They further suggested that the optical scale may reflect the scale of the interference pattern constrained by the electron inertial length λ_e.

Therefore, although a correspondence consistent with the dispersion relation may appear transiently when the background arc structure and peak frequency are stable (Figure 4 and the early phase of Figure 5), such behavior is not expected to persist in a statistical sense. Instead, the statistical result that flickering is concentrated within a relatively limited frequency range (4–12 Hz in this study), independent of patch size, can be naturally interpreted in terms of interference among multiple waves and the characteristic scale set by the electron inertial length.

Considering the present observations and the results of Yaegashi et al. (2011), it may be possible, at least during moments when both the background arc shape and the peak frequency are temporally stable, to estimate the modulation altitude of the electron flux from the patch size and the flickering frequency. For events such as Figure 4 and the early phase of Figure 5, the observed combination of the frequency peak and the apparent wave number (i.e., patch size) does not strongly conflict with

https://doi.org/10.5194/egusphere-2026-865
Preprint. Discussion started: 10 April 2026

the dispersion relation of O^+ EMIC waves. In such cases, a single wave mode may locally dominate, and interference among multiple modes may be relatively weak.

Under this assumption, the horizontal scale of the patches can be regarded as the ionospheric mapping of the electron inertial length in the region where electrons interact with the waves. The electron inertial length is given by $\lambda_e = c/\omega_{pe} \propto n_e^{-1/2}$. By adopting a model for the altitude profile of electron density and inverting this relationship, the approximate altitude of the modulation region may be inferred. The representative patch size obtained in this study, 4.4 km at an assumed altitude of 110 km, corresponds, when mapped to the auroral acceleration region, to an electron inertial length of order $\lambda_e \sim$ 100–400 m. This suggests that the optical scale of flickering patches may provide a useful diagnostic of the modulation altitude.

The corresponding electron density estimated from this inertial scale is on the order of $n_e \sim 3 \times 10^3\ \mathrm{cm}^{-3}$. This value appears somewhat high compared to typical electron densities for the auroral acceleration region (Rönnmark, 1999); however, it is not implausible if the modulation occurs near the lower boundary of the acceleration region or within a relatively dense plasma environment connected to the topside ionosphere.

In this study, we used wide-FoV observations with a diagonal fisheye lens to examine flickering aurora generation models that have previously been discussed mainly on the basis of narrow-field camera and photometer observations. This approach allows the investigation to be extended to mesoscales of several hundred kilometers. While earlier studies have investigated in detail the temporal evolution of individual patches, dispersion relations, and their correspondence with EMIC waves within localized FoV, mesoscale structures such as the spatial extent over which modulation at the same frequency band is maintained, or how wave sources with different peak frequencies are arranged relative to one another, have not been fully captured.

By covering a wide FoV simultaneously, this study demonstrates (1) how the presence or absence of flickering evolves toward substorm onset, (2) that multiple wave source regions can be aligned in the east–west direction, each exhibiting a distinct peak frequency while following the background auroral arc, and (3) that although the relationship between patch size and frequency can be locally consistent with the dispersion relation, it may not hold statistically due to the influence of wave interference. These results indicate that mesoscale observations of flickering aurora provide an effective diagnostic for understanding how the microscopic physics of EMIC growth, propagation, and resonant electron acceleration is influenced by the macroscopic dynamics of discrete auroral arc development and motion during substorms. In addition, diagonal-fisheye imaging provides access to off-zenith perspectives that may be useful for exploring apparent vertical structuring and motion, potentially offering further constraints on field-aligned development and emission-altitude variability. Future accumulation of wide-FoV, high-time-resolution observations under a range of geomagnetic activity levels is expected to further advance our understanding of the mesoscale structure and temporal evolution of EMIC acceleration regions as revealed through flickering aurora.

3 Conclusions

Using high-time resolution, wide-field imaging, we have characterized the mesoscale organization of flickering aurora over spatial scales of several hundred kilometers, placing previous narrow-field results into a broader mesoscale context. Flickering was observed intermittently in the 3–20 Hz range, with most power between 4 and 12 Hz, consistent with O^+ EMIC waves generated at altitudes of several thousand kilometers. The occurrence and visibility of flickering depended strongly on the evolution of the discrete arc: it disappeared as the background arc narrowed and intensified before substorm onset, while persisting on a wider polar-side discrete aurora and in the subsequent bulge, suggesting that suitable plasma and acceleration conditions are not simply controlled by brightness alone but also by the latitudinal width and structure of the arc. Spatial mapping revealed multiple frequency clusters along the same arc, separated by ∼150 km. These features indicate that multiple EMIC sources can coexist along neighboring field lines, each shaped by local plasma parameters and inverted-V potential structures, in line with interference-based models (Sakanoi et al., 2005; Gustavsson et al., 2008) and with beam-driven instability (Temerin and Lysak, 1984). Finally, although individual examples sometimes show an inverse relation between patch size and frequency reminiscent of the EMIC dispersion relation, our statistical analysis demonstrates that flickering frequencies are distributed within a similar band regardless of patch size, consistent with the idea that the optical scale reflects interference patterns rather than a simple one-to-one mapping from a single-mode dispersion curve.

Data availability. The raw files used in the analyses presented in this paper are available from Zenodo at https://doi.org/10.5281/zenodo.18481501 and https://doi.org/10.5281/zenodo.18537506.

Video supplement. Video 1 shows selected intervals of the flickering aurora observed at Poker Flat Research Range, Alaska, on 8 February 2016, obtained with the sCMOS camera used in this study. The video is available via the TIB AV-Portal at https://doi.org/10.5446/72336 (Nanjo, 2026).

Author contributions. SN performed all data analyses and prepared the manuscript. SK contributed to the conception of the study. TS contributed to the interpretation of the results. YM contributed to the observations, data management, and interpretation of the results. All authors contributed to revising the manuscript and approved the final version.

Competing interests. At least one of the (co-)authors is a member of the editorial board of Annales Geophysicae.

Acknowledgements. The authors thank Dr. Don Hampton, Dr. Yoko Fukuda and the staff at Poker Flat Research Range for operational support for the sCMOS camera observations. This work was carried out by the joint research program of Institute for Space–Earth Environmental Research, Nagoya University. This research has been supported by the Japan Society for the Promotion of Science (JSPS) (grant no. 25302006). The first author is a JSPS Overseas Research Fellow.

https://doi.org/10.5194/egusphere-2026-865
Preprint. Discussion started: 10 April 2026

References

Beach, R., Cresswell, G., Davis, T., Hallinan, T., and Sweet, L.: Flickering, a 10-cps fluctuation within bright auroras, Planetary and Space Science, 16, 1525–1529, https://doi.org/10.1016/0032-0633(68)90064-0, 1968.

Chen, L.-J., Kletzing, C. A., Hu, S., and Bounds, S. R.: Auroral electron dispersion below inverted-V energies: Resonant deceleration and acceleration by Alfvén waves, Journal of Geophysical Research: Space Physics, 110, https://doi.org/10.1029/2005JA011168, 2005.

Fukuda, Y., Kataoka, R., Uchida, H. A., Miyoshi, Y., Hampton, D., Shiokawa, K., Ebihara, Y., Whiter, D., Iwagami, N., and Seki, K.: First evidence of patchy flickering aurora modulated by multi-ion electromagnetic ion cyclotron waves, Geophysical Research Letters, 44, 3963–3970, https://doi.org/10.1002/2017GL072956, 2017.

Grydeland, T., Gustavsson, B., Baddeley, L., Lunde, J., and Blixt, E. M.: Conditional integration of Incoherent Scattering in relation to flickering aurora, Journal of Geophysical Research: Space Physics, 113, https://doi.org/10.1029/2008JA013039, 2008.

Gustavsson, B., Lunde, J., and Blixt, E. M.: Optical observations of flickering aurora and its spatiotemporal characteristics, Journal of Geophysical Research: Space Physics, 113, https://doi.org/10.1029/2008JA013515, 2008.

Kataoka, R., Miyoshi, Y., Sakanoi, T., Yaegashi, A., Ebihara, Y., and Shiokawa, K.: Ground-based multispectral high-speed imaging of flickering aurora, Geophysical Research Letters, 38, https://doi.org/10.1029/2011GL048317, 2011.

Kataoka, R., Fukuda, Y., Miyoshi, Y., Miyahara, H., Itoya, S., Ebihara, Y., Hampton, D., Dahlgren, H., Whiter, D., and Ivchenko, N.: Compound auroral micromorphology: ground-based high-speed imaging, Earth, Planets and Space, 67, 23, https://doi.org/10.1186/s40623-015-0190-6, 2015.

Kataoka, R., Chaston, C. C., Knudsen, D., Lynch, K. A., Lysak, R. L., Song, Y., Rankin, R., Murase, K., Sakanoi, T., Semeter, J., Watanabe, T.-H., and Whiter, D.: Small-Scale Dynamic Aurora, Space Science Reviews, 217, 17, https://doi.org/10.1007/s11214-021-00796-w, 2021.

Kunitake, M. and Oguti, T.: Spatial-Temporal Characteristics of Flickering Spots in Flickering Auroras, Journal of geomagnetism and geoelectricity, 36, 121–138, https://doi.org/10.5636/jgg.36.121, 1984.

Lin, C. S., Wong, H. K., Koga, J., and Burch, J. L.: Excitation of low-frequency waves by auroral electron beams, Journal of Geophysical Research: Space Physics, 94, 1327–1337, https://doi.org/10.1029/JA094iA02p01327, 1989.

Lund, E. J. and LaBelle, J.: On the generation and propagation of auroral electromagnetic ion cyclotron waves, Journal of Geophysical Research: Space Physics, 102, 17 241–17 253, https://doi.org/10.1029/97JA01455, 1997.

Lund, E. J., LaBelle, J., Torbert, R. B., Liou, K., Peria, W., Kletzing, C. A., Kelley, M. C., Baker, S. D., Primdahl, F., Stenbaek-Nielsen, H. C., Ranta, A., Haerendel, G., and Frey, H. U.: Observation of electromagnetic oxygen cyclotron waves in a flickering aurora, Geophysical Research Letters, 22, 2465–2468, https://doi.org/10.1029/95GL02409, 1995.

McFadden, J. P., Carlson, C. W., Boehm, M. H., and Hallinan, T. J.: Field-aligned electron flux oscillations that produce flickering aurora, Journal of Geophysical Research: Space Physics, 92, 11 133–11 148, https://doi.org/10.1029/JA092iA10p11133, 1987.

McHarg, M. G., Hampton, D. L., and Stenbaek-Nielsen, H. C.: Fast photometry of flickering in discrete auroral arcs, Geophysical Research Letters, 25, 2637–2640, https://doi.org/10.1029/98GL01972, 1998.

Michell, R. G., McHarg, M. G., Samara, M., and Hampton, D. L.: Spectral analysis of flickering aurora, Journal of Geophysical Research: Space Physics, 117, https://doi.org/10.1029/2011JA016703, 2012.

Nanjo, S.: Flickering Aurora Observed at Poker Flat Research Range, Alaska, on 8 February 2016, Swedish Institute of Space Physics (IRF), https://doi.org/10.5446/72336, https://doi.org/10.5446/72336, 2026.

Rönnmark, K.: Electron acceleration in the auroral current circuit, Geophysical Research Letters, 26, 983–986, https://doi.org/10.1029/1999GL900133, 1999.

Sakanoi, K. and Fukunishi, H.: Temporal and spatial structures of flickering aurora derived from high-speed imaging photometer observations at Syowa Station in the Antarctic, Journal of Geophysical Research: Space Physics, 109, https://doi.org/10.1029/2003JA010081, 2004.

Sakanoi, K., Fukunishi, H., and Kasahara, Y.: A possible generation mechanism of temporal and spatial structures of flickering aurora, Journal of Geophysical Research: Space Physics, 110, https://doi.org/10.1029/2004JA010549, 2005.

Temerin, M. and Lysak, R. L.: Electromagnetic ion cyclotron mode (ELF) waves generated by auroral electron precipitation, Journal of Geophysical Research: Space Physics, 89, 2849–2859, https://doi.org/10.1029/JA089iA05p02849, 1984.

Temerin, M., McFadden, J., Boehm, M., Carlson, C. W., and Lotko, W.: Production of flickering aurora and field-aligned electron flux by electromagnetic ion cyclotron waves, Journal of Geophysical Research: Space Physics, 91, 5769–5792, https://doi.org/10.1029/JA091iA05p05769, 1986.

Whiter, D. K., Lanchester, B. S., Gustavsson, B., Ivchenko, N., and Dahlgren, H.: Using multispectral optical observations to identify the acceleration mechanism responsible for flickering aurora, Journal of Geophysical Research: Space Physics, 115, https://doi.org/10.1029/2010JA015805, 2010.

Yaegashi, A., Sakanoi, T., Kataoka, R., Asamura, K., Miyoshi, Y., Sato, M., and Okano, S.: Spatial-temporal characteristics of flickering aurora as seen by high-speed EMCCD imaging observations, Journal of Geophysical Research: Space Physics, 116, https://doi.org/10.1029/2010JA016333, 2011.